

Automated Deepfake Detection

Ping Liu

Abstract—In this paper, we propose to utilize Automated Machine Learning to automatically search architecture for deepfake detection. Unlike previous works, our method benefits from the superior capability of deep learning while relieving us from the high labor cost in the manual network design process. It is experimentally proved that our proposed method not only outperforms previous non-deep learning methods but achieves comparable or even better prediction accuracy compared to previous deep learning methods. To improve the generality of our method, especially when training data and testing data are manipulated by different methods, we propose a multi-task strategy in our network learning process, making it estimate potential manipulation regions in given samples as well as predict whether the samples are real. Comparing to previous works using similar strategies, our method depends much less on prior knowledge, such as no need to know which manipulation method is utilized and whether it is utilized already. Extensive experimental results on two benchmark datasets demonstrate the effectiveness of our proposed method on deepfake detection.

Index Terms—Deepfake Detection, Neural Architecture Search, Potential Manipulation Region Localization.

I. INTRODUCTION

Deep fake detection aims to tell whether the face in a given image is synthesized (fake) by a modern computer graphics and computer vision technique or not (real). With the development of computer graphics and computer vision [1], [2], [3], [4], [5], [6], the generated faces become so visually realistic that it is difficult even for humans to differentiate. The unauthorized and malicious distribution of those fake images or videos brings serious concern among communities. Because of this, an efficient and effective solution for deepfake detection becomes necessary. In past three years, deep convolutional neural networks (CNNs) have been utilized for deepfake detection due to their promising performance in various computer vision applications, *e.g.*, fine-grained image classification [7], person counting [8], structural learning [9], person re-identification [10], [11], [12], semantic segmentation [13], [14], [15], and etc.

Most recent CNNs-based deepfake detection methods [16], [17], [18] are built on backbones for other computer vision tasks, such as image classifications (ResNet [16], XceptionNet [17]), or segmentation (U-Net [18]). While directly borrowing the networks originally designed for other tasks, *e.g.*, image classification, semantic segmentation, might relieve researchers from heavy labor cost in network design, it fails to consider the characteristics in deepfake detection. For example, image classification tasks [7] mainly focus on the shape, color, and semantic difference between different categories, while deepfake detection relies more on local textures,

especially feature discrepancies between different regions. In segmentation tasks [14], [15], the networks need to extract the high-level semantic features and capture contextual relations between distant pixels and regions, and thus they usually have a large model size and make the inference time-consuming. The large number of parameters and long inference time both limit their further application on low-resource systems, *e.g.*, iPhone, iPad, and etc., where the deepfake detection models might be deployed.

In [19], researchers manually design a convolutional neural architecture after analyzing the characteristics of deepfake detection. Specifically, they manually design a new architecture named Gram-Net to extract discriminative texture from given samples. This designed Gram-Net not only achieves promising performance in fake image detection but also facilitates to further interpret the results. However, as pointed out in previous works, manually design a neural architecture is never an easy task. In fact, a manual design process is usually time-consuming and labor expensive, especially when multiple constraints need to be considered at the same time, *e.g.*, limitations from accuracy, inference time, and model size.

To this end, we propose a method, which is called Automated Deepfake Detection (ADD), to construct a neural architecture for deepfake detection in an adaptive and automatic manner. To the best of our knowledge, it is the first method that utilizes automated machine learning (AutoML) for deepfake detection. As shown in Fig.1, thanks for the AutoML [20], [21], ADD is able to relieve us from the heavy labor cost during manual network design processes, while still achieving a good balance between prediction accuracy and network sizes. To further improve the generality of our searched network for deepfake detection, we additionally introduce a multi-task strategy to our ADD architecture learning process. Specifically, there are two tasks conducted simultaneously in our ADD, *i.e.*, locating potential manipulated regions (even when no manipulation occurs), and differentiating fake samples from real ones. Explicitly locating manipulated regions has two advantages in the deepfake detection task, we believe. On the one hand, it is able to let the network focus on the features extracted in those potential regions and depress the irrelevant information from other places; on the other hand, explicitly localizing the manipulated regions benefits the downstream interpretation. Our experimental results empirically prove that our ADD with a multi-task strategy can bring significant performance improvement in cross data evaluations (Table. V and VI).

Although two recent fake image detection works [18], [22] also point out the advantages of explicitly detecting manipulated regions, there are significant differences between their proposed methods and ADD: (1) [18], [22] directly borrow networks manually designed for image classification or segmentation, and apply them for deepfake detection, while

P. Liu is with Institute of High Performance Computing, Agency for Science, Technology, and Research, Singapore.

Manuscript received Jan 22, 2021.

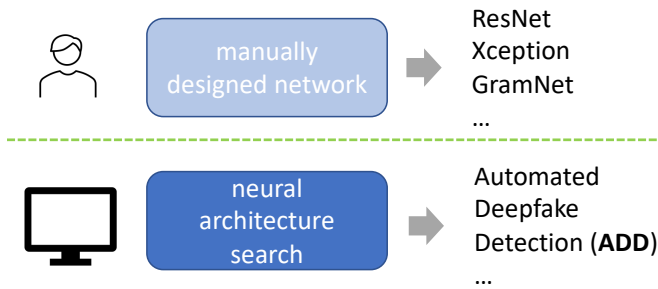


Fig. 1: The difference between previous deepfake detection methods. Previous works utilize manually designed network for deepfake detection, while in this submission, we conduct neural architecture search to construct a deep network for deepfake detection.

ADD utilizes a gradient update method to automatically search an architecture for deepfake detection; (2) [18], [22] need strong prior knowledge to generate ground truth maps to indicate manipulation regions, for example, which kind of manipulation is utilized to generate the fake images. In their method, different manipulation methods correspond to different manipulation regions: the manipulated region is around the whole face in manipulation methods focusing on swapping whole faces, while in an expression transfer method, [18], [22] set the manipulated regions around the mouth only. The heavy dependence on prior knowledge limits the generalization of their methods [18], [22], since in real scenarios, we might not know which manipulation method is utilized for the given samples. On the contrary, our method does not need to know which manipulated method is utilized; (3) [22] introduces an additional facial expression recognition branch to detect fake images with facial expression swapped. The introduced module not only limits the generality of [22] but also brings additional computational cost.

In summary, our contributions are listed as follows:

(1) This is the first work to automatically search neural architectures for deepfake detection. Comparing to previous works, our method significantly decreases the dependence on human expertise in network design, while still keeping a good performance on prediction accuracy.

(2) We integrate a multi-task strategy into our automated deepfake detection method. The integration strategy not only predicts the real or fake for each given instance, but also tries to locate the potential manipulated region in each sample. Because of this strategy, our network can focus more on the features extracted from those potentially manipulated regions. The performance improvement in the cross-domain evaluation experimentally demonstrates the efficacy of this strategy, especially when testing data and training data are manipulated by different methods.

(3) We conduct extensive experiments on two challenging datasets for deepfakes, *i.e.*, FaceForensics++ [23] and CelebDF [24]. The performance on in-domain and cross-domain evaluations both demonstrate the effectiveness of our proposed method.

II. RELATED WORK

In this section, we will briefly survey previous works related to this submission, including deepfake detection and neural architecture search.

A. Deepfake Detection

Deepfake is a kind of synthetic media, where the human face in the original data (real) is replaced with others' faces, or the human face attribute is replaced with others' face attribute. By leveraging the latest computer graphics technologies and generative machine learning methods [25], [26], [27], [28], [29], [30], the generated deepfake is of high quality and hard to distinguish even for human observers. In past years, a variety of works for deepfake detection have been proposed, most of which treat deepfake detection as a vanilla binary image classification problem, *i.e.*, distinguish the real samples from the fake samples. As an initial attempt, [31], [32] propose to utilize handcrafted features and steganalysis in their works. With the development of CNNs and their application in computer vision communities, researchers propose various CNN-based works for deepfake detection [33], [23], [34], [35]. The initial works based on CNNs, such as [33], [23], [34], [35], directly utilize networks whose efficacy has been proved in image classification tasks. [33] builds a CNN based on inception modules [36] and trains the constructed network under a supervision of a mean squared error loss. [23] transfers XceptionNet [17] from image classification to deepfake detection by simply modifying the output layer. [34] construct a two-branch structure for deepfake detection, one of which is a GoogLeNet [37] pretrained on ImageNet. [35] presents a method based on Capsule network [38] for deepfake detection. [33], [23], [34], [35] treat deepfake detection as a vanilla binary classification problem, with few considerations about the differences between natural image classification and deepfake detection.

Recently, [39], [40], [22], [41] analyze the unique characteristics of deepfake and correspondingly propose their solutions from a new point of view. In [39], [40], [22], other than predicting the real or fake for each sample, the position of the manipulated region is also estimated by the network. By treating the region localization as a segmentation task, [39], [40], [22] build their work based on the backbones originally proposed for segmentation, such as U-Net [39], Encoder-Decoder structure [22]. [24] build their work on XceptionNet, however, unlike [17], [24] localizes the blending boundaries existing in fake samples as well as the real/fake labels. [24] believes that the blending boundary, which is named face X-ray, exists if a Poisson blending is utilized for a post-process. The location of the face X-ray not only can tell us whether the face is manipulated but also where it is manipulated. However, to achieve this goal, [24] needs external data collection and annotation to train their model. For a systematic review for deepfake generation and detection, please refer to [42].

B. Automated Machine Learning and Neural Architecture Search

Automated machine learning (AutoML) is a research topic focusing on automating the aspects in machine learning tasks, such as neural architecture construction, hyperparameter setting, data augmentation policies setting, and etc. Neural architecture search (NAS), as one sub-research area of AutoML, aims to automatically search and build a neural architecture based on given tasks and data. In an ideal case, NAS is expected to decrease the dependence on human expertise in the network design process [41], [39], [40], [22] for target tasks. In past years, the efficacy of NAS has been successfully proved in various applications, *e.g.*, image classification [43], semantic segmentation [44], object detection [45], pose estimation [46], image super-resolution [47]. Generally, NAS conducts the architecture search in an iterative manner. In each iteration, good candidate solutions are selected and updated for the following iterations, while poor candidate solutions are dropped without further process. The search and update operation continues iteratively until the searched candidates achieve satisfactory performance on the training dataset. Based on the characteristics of the selection and update algorithms, previous works on NAS can be categorized into two major groups: reinforcement learning-based methods such as [48], and gradient-based methods such as [21], [20]. In those reinforcement learning-based works, searched candidates are utilized to evaluate on a validation set. The evaluation performance is leveraged to decide whether the searched candidates are on the correct track. For example, [48] utilizes the validation accuracy to indicate whether the candidate architecture searched at the moment is in the right direction or not. Although those reinforcement learning-based methods have been proved effective in a variety of works [48], the training difficulty and huge computation cost limit their applications comparing to their counterpart [21], [20]. In [21], [20], they propose a gradient update method to speed up the whole search process. The basic idea of gradient-based NAS works [21], [20] is to utilize a continuous relaxation of the architecture representation, making the learning process can be updated using gradient descent methods. Compared to the reinforcement learning-based methods [48], gradient update based methods [21], [20] can conduct the whole search process in an efficient and stable manner.

III. METHODOLOGY

In this section, we describe the technical details of our automated deepfake detection. At first, we introduce the preliminary knowledge of NAS in Sec. III-A; at second, in Sec. III-B, we discuss our search space; at third, we illustrate our multi-task automated settings, *i.e.*, differentiating real samples from fake samples and locating potential manipulated regions simultaneously.

A. Preliminaries

In this work, we follow previous NAS works [20], [21], which are conducting in a micro-search manner. In the micro-search works such as [20], [21], the target is to discover a

neural cell and hierarchically stack this searched neural cell based on a pre-defined structure. Comparing to its counterpart, *i.e.*, the macro-search methods which directly discover the entire network architecture, the micro-search methods can reduce the search cost significantly.

In micro-search methods [20], [21], the searched cell is viewed as a directed acyclic graph, in which each node is a block of operations. For each block, it receives two feature tensors as its input, conducts two selected operations for the two input tensor respectively, and then sum those two processed tensors. The operations to process the feature tensors are selected from a pre-defined operation set, which is known as *search space*. The search space includes a variety of pre-specified operations, such as max pooling with different kernel sizes, average pooling with different kernel sizes, convolution with different kernel sizes, and etc. Specifically, for the i_{th} block in the c_{th} cell, if we denote the two input tensors as $I_{i,1}^c$ and $I_{i,2}^c$, the two corresponding operations selected as $OP_{i,1}^c(*)$ and $OP_{i,2}^c(*)$, then the output tensor of the i_{th} block in the c_{th} cell, denoted as O_i^c , can be defined by:

$$O_i^c = OP_{i,1}^c(I_{i,1}^c) + OP_{i,2}^c(I_{i,2}^c) \quad (1)$$

where $I_{i,1}^c$ and $I_{i,2}^c$ are two input tensors. It is noted that $I_{i,1}^c$ and $I_{i,2}^c$ are output tensors from the previous neural cells, *i.e.*, O_{*}^{c-1} and O_{*}^{c-2} .

As pointed out by previous works [], the keys of their success is how to define an optimal search space and how to find an optimal choice, *i.e.*, $OP_{i,1}^c(*)$ and $OP_{i,2}^c(*)$ from the search space, to process input feature tensors for generating an output feature tensor, which is utilized as an input tensor for the following block. The operation selection process is a categorical process in principle. Previous works such as [48], solve this categorical choice problem by reinforcement learning but have to face the training difficulty and high computational cost. While in our work, by following [20], [21], we choose a more efficient strategy: relaxing the categorical choice of a particular operation as a Softmax process over all possible operations, which is defined as:

$$OP_{i,1}^c(I_{i,1}^c) = \sum_{H \in I_i^c} \sum_{op \in OP} \frac{\exp(\alpha_{op}^{H,i})}{\sum_{op' \in OP} \exp(\alpha_{op'}^{H,i})} op(H) \quad (2)$$

in which architecture parameters $\alpha = \{\alpha_{op}^{H,i}\}$ represents the topology structure for the searched cell, *e.g.*, which operations are selected in the corresponding block. For all selected operations, their parameters are denoted as w . And therefore, to search a neural cell, there are two groups of parameters need to be learned: architecture parameter α and operation parameter w . The training loss is defined as follows:

$$L(x, y) = loss(y|x; \alpha, w) \quad (3)$$

in which x denotes data samples, y denotes the corresponding labels, $loss$ denotes a discrepancy measure function (*e.g.*, cross-entropy), α denotes the architecture parameters, w denotes the associated weights corresponding to α .

By the relaxation strategy proposed in [20], [21], the architecture parameter α and operation parameter w can be learned in an alternative manner. Specifically, the architecture

parameter α is trained on the validation set while the operation parameter w is trained on the training set. During the training, the two sets of parameters can be updated by gradient descent, which runs in a high efficiency. After training, the one in I_i^c with the maximum value, *i.e.*, $\max \frac{\exp \alpha_{op}^{H,i}}{\sum \exp(\alpha_{op}^{H,i})}$, is selected as $I_{i1}^c(*)$, and the operation with the maximum weight is selected as $OP_{i1}^c(*)$. The whole training process is shown in Alg. 1.

Algorithm 1: Searching Algorithm

Input: a training set D_{train} , a validation set D_{val} randomly initialized α , random initialized w

Output: optimized parameter α^* and w^*

- 1 **while** *not converged* **do**
 - 2 sample a batch of data from the training set, denoted as $d_{train,b}$, where b is the batch index;
 - 3 calculate loss L_T based on Eq. 3 by $d_{train,b}$;
 - 4 update operation parameter w by gradient descent: $w = w - \nabla_w L_T$;
 - 5 sample a batch of data from the validation set, denoted as $d_{val,b}$, where b is the batch index;
 - 6 calculate loss L_V based on Eq. 3 by $d_{val,b}$;
 - 7 update architecture parameter α by gradient descent: $\alpha = \alpha - \nabla_\alpha L_V$
-

B. Search for Deepfake Detection

Search Space and Network Structure The macro structure of our deepfake detection backbone is similar with ResNet. We replace the residual layer with the neural cell found by our algorithm. The operations in the searched neural cell are selected from a pre-specified search space, which includes:

- zero operation;
- identity mapping;
- 3x3 convolution;
- 3x3 depth-wise separable convolution;
- 3x3 dilated convolution;
- 5x5 convolution;
- 5x5 depth-wise separable convolution;
- 5x5 dilated convolution;
- 7x7 convolution;
- 7x7 depth-wise separable convolutions

We construct the search space based on the following considerations: (1) vanilla convolution operations are proved effective in the previous classification works; (2) previous human-designed network for deepfake detection, such as [49], [23], proved the efficacy of depth-wise separable convolution; (3) dilated convolution is utilized to enlarge the receptive field of the constructed network.

The searched cell, which is consisted of the operations selected from our search space, constructs a deep architecture based on the similar macro structure of ResNet. Specifically, we replace each residual block in ResNet with our searched cell. For sample x_i , we feed it to the searched architecture and denote the extracted feature from the highest layer as $g_i \in \mathbb{R}^{800 \times w' \times h'}$. The extracted feature g_i is feed to a 1×1 convolution layer and two full connection layers to generate

logits, which is denoted as $h_i \in \mathbb{R}^2$. The dimension of the logits is 2 since the number of the target classes is 2, *i.e.*, real or fake.

Given the calculated logits h_* for each sample, our architecture is trained under a cross-entropy (CE) loss defined as:

$$\begin{aligned} L_{CE} &= \frac{1}{N} \sum_i \text{crossentropy}(h_i, y_i) \\ &= \frac{1}{N} \sum_i \text{crossentropy}(fc(g_i), y_i) \end{aligned} \quad (4)$$

where h_i denotes the logits for sample x_i , y_i is the ground truth label, fc denotes a full connection layer used to map g_i to logits h_i , N is the sample number.

C. Potential Manipulated Region Localization

In deepfake detection, the manipulated regions are located on faces, implying that the key information relevant to deepfake detection should be located on face regions rather than the background. More than that, previous face analysis works such as [50] point out that not all facial regions make the contribution to the target task. As a matter of fact, some facial regions might make more contributions than other regions for the target task. And therefore, utilize features extracted from all image regions without different focus might be sub-optimal.

Inspired by this, we propose to utilize an additional supervisory signal to make our searched architecture focus on the important regions for deepfake detection. Specifically, for sample x_i , we feed its extracted feature g_i to another 1×1 convolution layer to decrease its channel dimension to 1, which is denoted as $q_i \in \mathbb{R}^{1 \times w' \times h'}$. q_i is feed to a bi-linear up-sampling layer to reset the width and height, generating a mask denoted as $m_i \in \mathbb{R}^{1 \times w \times h}$, where w and h are the width and height for sample x_i . Since we want our network to focus on the potential manipulated regions in each image, specifically, the region on faces, we make the predicted m_i have high values on face regions and lower values on non-face regions. To generate the ground truth for m_i , we use a lightweight face detector provided by OpenCV to detect the face regions and generate a ground truth mask denoted as M_i . Concretely, we use an OpenCV face detector to detect a face in sample x_i , extract the landmarks on the detected face. The extracted landmarks are utilized to generate a convex hull. The ground truth mask M_i is generated by setting all the pixels inside the convex hull as one, and all the pixels outside the convex hull as zero. We train our model by additional supervision: minimizing the discrepancy between m_i and M_i by a mean square error (mse) loss:

$$L_{MSE} = \frac{1}{N} \sum_i \text{mse}(m_i, M_i) \quad (5)$$

where m_i denotes the predicted potential manipulated region for a sample x_i , M_i is the ground truth, N is the sample number.

It should be noted that the predicted potential manipulated region m_i in our work is different from the predicted mask s_i in previous works such as [22]. In [22], the value of each pixel s_i is between 0 and 1, indicating *whether* or not a manipulation

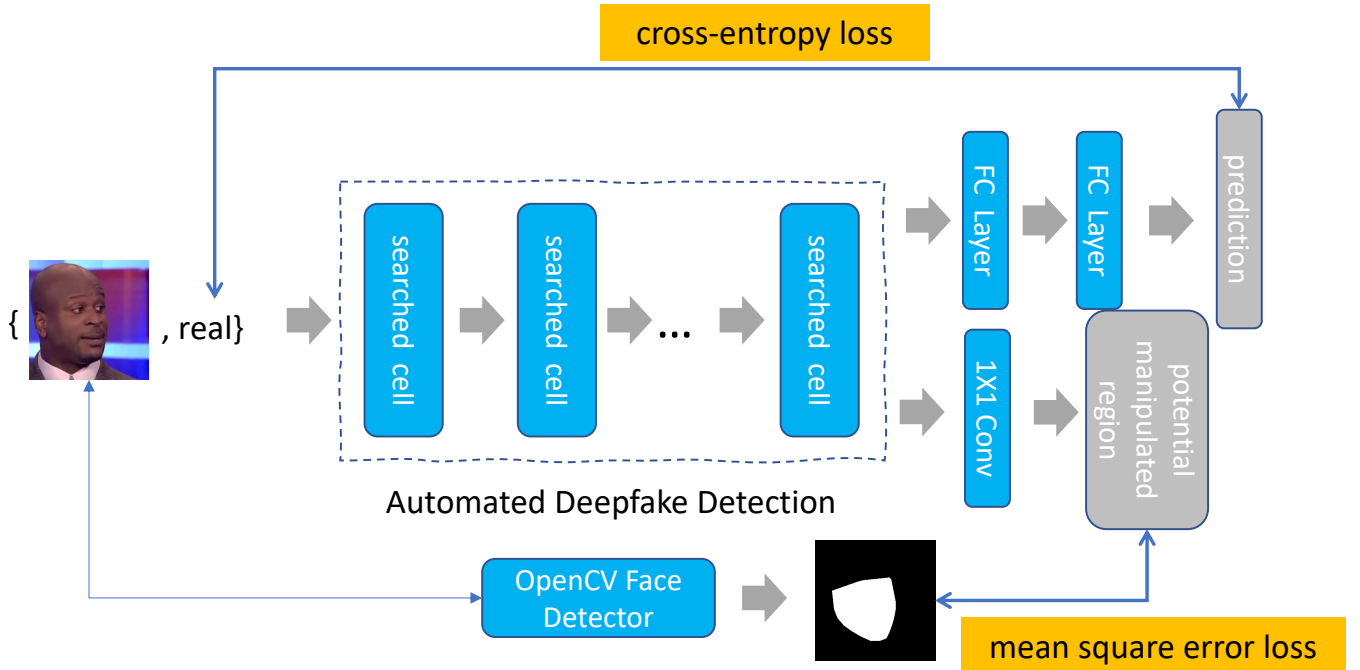


Fig. 2: The pipeline of automated deepfake detection method.

exists in the sample; while in our work, the value of each pixel on the mask indicates *where* a manipulation *might* exist in the sample. In other words, the values of the mask s_i in [22] indicates whether a manipulation is applied to the corresponding sample; while the values of m_i in our work tells us where a manipulation method might be applied, with no need to know whether a manipulation method is applied already or which manipulation method is applied.

After introducing m_i , the loss term 4 is changed to:

$$\begin{aligned} L_{CE'} &= \frac{1}{N} \sum_i \text{crossentropy}(h_i \odot m_i, y_i) \\ &= \frac{1}{N} \sum_i \text{crossentropy}(fc(g_i \odot m_i), y_i) \end{aligned} \quad (6)$$

where \odot indicates an element-wise multiplication, g_i denotes the extracted feature for sample x_i , m_i denotes the estimated potential manipulation region in sample x_i , y_i is the ground truth label, N is the sample number.

D. Objective Function and Overall Algorithm

The total loss function need to optimize to learn an automated deepfake detector is defined as follows:

$$L_{overall} = L_{CE'} + \alpha * L_{MSE} \quad (7)$$

where $L_{CE'}$ is defined in Eq. 6, L_{MSE} is defined in Eq. 5, α is a parameter to balance contributions of the two loss terms. The overall pipeline is shown in Fig. 2.

IV. EXPERIMENTS

In this section, we evaluate our proposed method on two deepfake detection datasets. We first illustrate the dataset details in Sec. IV-A, implementation details and evaluation settings in Sec. IV-B. In Sec. IV-C, we compare our method with previous works on two benchmark datasets we test. The ablation study and discussion are illustrated in Sec. IV-D.

A. Datasets

We test our method on two benchmark datasets, including FaceForensics++ [23], Celeb-DF [24].

FaceForensics++ [23] has four different types of face manipulation methods: Face2Face [51], NeuralTextures [52], FaceSwap [53], and DeepFakes [54]. For each manipulation method, there are 1,000 real videos and 1,000 fake videos, which are split into 720 videos for training, 140 videos for validation, 140 videos for testing. In the four manipulation methods, Face2Face and FaceSwap are computer graphics-based methods, while NeuralTextures and Deepfakes are learning-based approaches.

- Face2Face [51] proposes a facial reenactment method to transfer expressions from a source video to a target video without changing the identity of the person in target videos.
- NeuralTextures [52] utilizes a rendering approach to conduct facial reenactments. It uses a photometric reconstruction loss as well as an adversarial loss to train a rendering network. The trained network modifies the facial expression of the person in a target video. It should

be noted that in NeuralTextures only the mouth region is modified, while other regions remain unchanged.

- FaceSwap [53] transfers the face region from a source video to the corresponding region in a target video. At first, FaceSwap fits a 3D template model based on extracted facial landmarks in a source video; then it back-projects the model to the target image by minimizing the shape difference. To make the result realistic, image blending and color correction are utilized.
- DeepFakes [54] conducts face replacement based on deep learning, in which an encoder-decoder structure is utilized. An encoder and a decoder, which are trained to reconstruct training images of the source videos, are applied to the target faces. A Poisson blending process is utilized to post-process the output.

Celeb-DF [24] is a new dataset with improved visual qualities. The celeb-DF dataset has 590 real videos and 5,639 fake videos in total. The real videos are collected from YouTube, which has 59 different celebrities. It is generated using advanced DeepFake synthesis techniques, and the generated results are post-processed to correct color mismatch, temporal flickering, making the generated results with better visual qualities.

Some examples from Face2Face [51], NeuralTextures [52], FaceSwap [53], DeepFakes [54], and Celeb-DF [24] are shown in Fig. 3.

B. Implementation Details and Evaluation Settings

We use an OpenCV face detector to coarsely locate the face from each image. The face region is cropped and resized to 256×256 . In the neural cell search process, we set the batch size as 8, the total epoch number as 300. To optimize the architecture parameter α , we use Adam optimizer and initialize it with a learning rate of 0.02. The learning rate is decayed by 10 at 60th and 150th epoch. To optimize the operation parameter w , we use a momentum SGD with a momentum value of 0.9. We set the learning rate to 0.1 and decrease it by a cosine scheduler. For both SGD and Adam optimizer, the weight decay number is set as 0.0005.

After searching the neural cell, we use it to construct a deep architecture whose parameters can be further refined. In this stage, we set the batch size as 96, the learning rate as 0.25, the epoch number as 300. An Adam optimizer with a momentum value of 0.9 and a weight decay of 0.0005 is utilized. We decay the learning rate by 10 at the 80th and 140th epochs.

We test our searched architecture under two evaluation settings, *i.e.*, inner-dataset evaluation and cross-dataset evaluation. In an inner-dataset evaluation, the training set and testing set are manipulated by the same method, while in a cross-dataset evaluation, the training set and testing set are manipulated by two different methods. The cross-dataset evaluation scenario is more practical since usually we do not know by what method the test image is manipulated.

We make a comparison with those previous works utilizing the same or similar experimental setting:

- Steg+SVM [55] is based on handcrafted features and a linear support vector machine classifier.

- Cozzolino [56] extends Steg+SVM [55] by combining the hand-crafted features utilized in [55] with a convolutional neural network.
- Bayar [57] manually designs a convolutional neural network consisted of convolutional layers, max-pooling layers, and fully-connection layers.
- Rahmouni [58] also proposes a convolutional neural architecture to extract features for deepfake detection.
- MseoNet [59] utilizes InceptionNet for detecting fake images. There are two inception modules in its architecture. The network is trained using a mean squared error between ground truth and prediction.
- XceptionNet [23] uses an XceptionNet which was manually designed for natural image classification. This architecture is constructed by inception-wise modules, in which depthwise separable convolution is utilized.
- LAE [39] utilizes an encoder-decoder network for simultaneously predicting real and fake labels as well as locating the manipulated regions.

We do not compare our work with Face X-ray [41] since it needs external data collection and annotation for training their network; we do compare our work with [22], [60] since they conduct additional inference task other than real/fake prediction and manipulation mask segmentation, and therefore bring additional computation cost and increase network complexity. For example, [22] brings a facial expression recognition module into their architecture to recognize facial expressions, [60] conducts a multilevel facial semantic segmentation in their architecture.

C. Comparison

Inner-dataset evaluation. The performance comparison under the inner-dataset setting is shown in Table. I-Table. IV. The performance comparisons on FF++ dataset with previous works under the same or similar setting are shown in Table. I: Deepfakes, Table. II: Face2Face, Table. III: FaceSwap, and Table. IV: NeuralTexutre. From the tables, we can find that our method (ADD) outperforms previous non-deep learning methods like Steg+SVM [55] and Cozzolino [56] by a large margin (10% \sim 20%). Compared to Bayar [57], Rahmouni [58], MseoNet [59], our ADD still achieves a higher performance (5% \sim 10%) on all four manipulation methods. LAE [39] is a work most similar to ADD since it tries to localize the manipulation regions. However, we can find that its performance is much lower than ADD (92.14% v.s. 98.33%). The better performance demonstrates the efficacy of the architecture searched by ADD. Among all the listed previous works, ADD is only outperformed a bit by XceptionNet [23]. In the four manipulation methods, ADD is a little outperformed by XceptionNet on Deepfakes, Face2Face, and FaceSwap. We assume that the performance difference between ADD and XceptionNet comes from the larger model size of XceptionNet. As shown in Table. VII, XceptionNet has a 80 MB model size and ADD has only a 45MB model size. A model with a deeper architecture and larger parameter size, as demonstrated in previous works, usually brings performance improvement significantly.



Fig. 3: Examples of Celeb-DF [24], FaceSwap [53], DeepFakes [54], Face2Face [51], and NeuralTextures [52] .

In Table. VII, we conduct an evaluation on CelebDF dataset and report the performance comparison. CelebDF dataset provides a validation list. We utilize the samples on the validation list as training samples, train five representative convolutional neural architectures, including ResNet-18, ResNet-152, VGG-16, and XceptionNet. From the table, we can find that the searched architecture by ADD outperforms ResNet-18 and ResNet-34, which has a smaller or similar model size. Comparing to ResNet-152 and VGG-16, our method still achieves a comparable performance but with a much smaller model size.

Method	Year	ACC
Steg+SVM [55]	2012	77.12%
Cozzolino [56]	2017	81.78%
Bayar [57]	2016	90.18%
Rahmouni [58]	2017	82.16%
MseoNet [59]	2018	95.26%
XceptionNet [23]	2019	98.85%
ADD	2021	97.45%

TABLE I: Result comparisons on Deepfakes.

Method	Year	ACC
Steg+SVM [55]	2012	74.68%
Cozzolino [56]	2017	85.32%
Bayar [57]	2016	94.93%
Rahmouni [58]	2017	93.48%
MseoNet [59]	2018	95.84%
XceptionNet [23]	2019	98.36%
LAE [39]	2020	92.14%
ADD	2021	98.33%

TABLE II: Result comparisons on Face2Face.

Cross-dataset evaluation. The performance comparison under the cross-dataset setting is shown in Table. V and Table. VI. Cross-dataset evaluation is more practical since in real scenarios, it is unknown which manipulation method is applied to testing data. To make a comparison with previous works, we follow previous cross-dataset evaluation settings: (1) train on Face2Face and test on FaceSwap; (2) train on FF++ and test on CelebDF. In both cases, our ADD outperforms previous works by a large margin, which demonstrates the better generality of

Method	Year	ACC
Steg+SVM [55]	2012	79.51%
Cozzolino [56]	2017	85.69%
Bayar [57]	2016	93.14%
Rahmouni [58]	2017	92.51%
MseoNet [59]	2018	93.43%
XceptionNet [23]	2019	98.23%
ADD	2021	97.20%

TABLE III: Result comparisons on FaceSwap.

Method	Year	ACC
Steg+SVM [55]	2012	76.94%
Cozzolino [56]	2017	80.60%
Bayar [57]	2016	86.04%
Rahmouni [58]	2017	75.18%
MseoNet [59]	2018	85.96%
XceptionNet [23]	2019	94.5%
ADD	2021	90.84%

TABLE IV: Result comparisons on NeuralTexture.

the architecture searched by our method.

Method	Year	Source	Target	ACC
MseoNet [59]	2018	Face2Face	FaceSwap	47.32%
XceptionNet [23]	2019	Face2Face	FaceSwap	49.94%
LAE [39]	2020	Face2Face	FaceSwap	63.15%
ADD	2021	Face2Face	FaceSwap	67.02%

TABLE V: Cross-dataset evaluation results. Train on Face2Face and test on FaceSwap.

D. Ablation Study

Efficacy of potential manipulation region estimation By setting α as zero or not, we conduct a performance comparison on cross-dataset evaluations to demonstrate the efficacy of learning potential manipulation regions. The performance comparison is illustrated in Table. VIII. From the table, we can find that the performance with L_{MSE} is much higher than the performance without L_{MSE} . This indicates the efficacy and necessity of learning the potential manipulation regions in ADD.

Method	Year	Source	Target	AUC
MseoNet [59]	2018	FF++	CelebDF	54.8%
XceptionNet [23]	2019	FF++	CelebDF	65.3%
Capsule [35]	2019	FF++	CelebDF	57.5%
ADD	2021	FF++	CelebDF	66.48%

TABLE VI: Cross-dataset evaluation results. Train on FF++ training set and test on CelebDF.

-	ResNet-18	ResNet152	VGG-16	XceptionNet	ADD
ACC	96.76%	98.30%	97.88%	96.32%	97.57%
Size(MB)	43	223	513	80	45

TABLE VII: Accuracy and model size comparison on CelebDF.

Method	Source	Target	ACC
w/o L_{MSE}	FF++	CelebDF	64.81%
w L_{MSE}	FF++	CelebDF	69.19%
w/o L_{MSE}	Face2Face	FaceSwap	57.22%
w L_{MSE}	Face2Face	FaceSwap	67.02%

TABLE VIII: Results compassion between w and w/o L_{MSE} .

Comparison of different learning rates We conduct a performance comparison between different learning rates. Specifically, by setting the learning rate as 0.5, 0.25, 0.01, batch size as 96, we trained our searched architecture on Deepfakes [54]. The performance comparison is shown in Fig. 4. From Fig. 4, we can find that the performance is stable with different learning rates, without a drastic fluctuation.

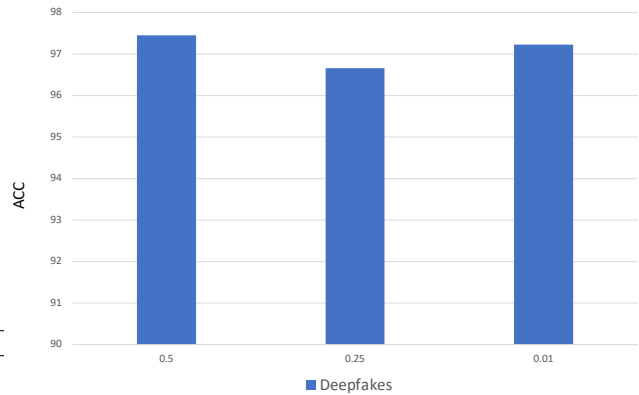


Fig. 4: Performance comparison with different learning rates on Deepfakes [54].

V. CONCLUSION

In this article, we propose to utilize automated machine learning to automatically construct a neural architecture for deepfake detection. To the best of our knowledge, this is the first time to apply AutoML in this research topic. It is experimentally proved that our searched architecture not only outperforms previous non-deep learning methods, but also achieves superior performance comparing to previous deep learning methods at most times. To improve the generality of our method, we integrate a multi-task strategy in our network construction process, making it estimate the potential manipulation regions as well as predict the real or fake labels. This strategy can have the network focus more on the regions might be manipulated. Comparing to previous works, our potential manipulation regions depends few on prior knowledge, e.g., no need to know which manipulation methods is utilized or whether it is utilized. Experimental results on two benchmark datasets, manipulated by five different methods, have demonstrated the efficacy of our proposed method, especially when testing data and training data are manipulated by different methods. In the future, we plan to explore more advanced search methods and search spaces to further improve the prediction ability of our method.

VI. ACKNOWLEDGEMENTS

This work was supported by the Agency for Science, Technology and Research (A*STAR) under AI and ANALYTICS SEED GRANT (Grant No. Z20F3RE005) and AME Programmatic Funding Scheme (Project No. A18A1b0045).

REFERENCES

- [1] R. Abdal, Y. Qin, and P. Wonka, "Image2stylegan: How to embed images into the stylegan latent space?" in *ICCV*, 2019.
- [2] T. Karras, S. Laine, M. Aittala, J. Hellsten, J. Lehtinen, and T. Aila, "Analyzing and improving the image quality of stylegan," in *CVPR*, 2020.
- [3] P.-W. Wu, Y.-J. Lin, C.-H. Chang, E. Y. Chang, and S.-W. Liao, "Relgan: Multi-domain image-to-image translation via relative attributes," in *ICCV*, 2019.
- [4] Y. Shi, X. Zhou, P. Liu, and I. W. Tsang, "Generative transition mechanism to image-to-image translation via encoded transformation," *CoRR*, 2021.
- [5] B. Hu, Z. Zheng, P. Liu, W. Yang, and M. Ren, "Unsupervised eyeglasses removal in the wild," *IEEE Transactions on Cybernetics*, 2020.
- [6] Y. Zhang, I. W. Tsang, J. Li, P. Liu, X. Lu, and X. Yu, "Face hallucination with finishing touches," *IEEE Transactions on Image Processing*, 2021.
- [7] H. Fan, P. Liu, M. Xu, and Y. Yang, "Unsupervised visual representation learning via dual-level progressive similar instance selection," *IEEE Transactions on Cybernetics*, 2021.
- [8] J. Zhou, L. Zhang, D. Jiawei, X. Peng, Z. Fang, Z. Xiao, and H. Zhu, "Locality-aware crowd counting," *IEEE Transactions on Pattern Analysis and Machine Intelligence*, 2021.
- [9] P. Pan, P. Liu, Y. Yan, T. Yang, and Y. Yang, "Adversarial localized energy network for structured prediction," in *AAAI Conference on Artificial Intelligence*, 2020.
- [10] J. Miao, Y. Wu, P. Liu, Y. Ding, and Y. Yang, "Pose-guided feature alignment for occluded person re-identification," in *ICCV*, 2019.
- [11] Z. Zheng and Y. Yang, "Rectifying Pseudo Label Learning via Uncertainty Estimation for Domain Adaptive Semantic Segmentation," *International Journal of Computer Vision*, 2021.
- [12] Z. Zhong, L. Zheng, Z. Zheng, S. Li, and Y. Yang, "Camstyle: A novel data augmentation method for person re-identification," *IEEE Transactions on Image Processing*, 2019.
- [13] Y. Luo, Z. Zheng, L. Zheng, T. Guan, J. Yu, and Y. Yang, "Macro-micro adversarial network for human parsing," in *European Conference on Computer Vision*, 2018.
- [14] Y. Luo, P. Liu, T. Guan, J. Yu, and Y. Yang, "Significance-aware information bottleneck for domain adaptive semantic segmentation," in *International Conference on Computer Vision*, 2019.
- [15] —, "Adversarial style mining for one-shot unsupervised domain adaptation," in *Advances in Neural Information Processing Systems*, 2020.
- [16] K. He, X. Zhang, S. Ren, and J. Sun, "Deep residual learning for image recognition," in *IEEE Conference on Computer Vision and Pattern Recognition*, 2016.
- [17] F. Chollet, "Xception: Deep learning with depthwise separable convolutions," in *CVPR*, 2017.
- [18] M. Du, S. Pentyala, Y. Li, and X. Hu, "Towards Generalizable Forgery Detection with Locality-aware AutoEncoder," in *CIKM*, 2020.
- [19] Z. Liu, X. Qi, and P. H. Torr, "Global texture enhancement for fake face detection in the wild," in *CVPR*, 2020.
- [20] H. Liu, K. Simonyan, and Y. Yang, "Darts: Differentiable architecture search," in *ICLR*, 2019.
- [21] X. Dong and Y. Yang, "Searching for a robust neural architecture in four gpu hours," in *CVPR*, 2019.
- [22] G. Mazaheri and A. K. Roy-Chowdhury, "Detection and Localization of Facial Expression Manipulations," *arXiv*, 2021.
- [23] A. Rossler, D. Cozzolino, L. Verdoliva, C. Riess, J. Thies, and M. Niessner, "FaceForensics++: Learning to detect manipulated facial images," in *ICCV*, 2019.
- [24] Y. Li, X. Yang, P. Sun, H. Qi, and S. Lyu, "Celeb-DF : A Large-scale Challenging Dataset for DeepFake Forensics," in *CVPR*, 2020.
- [25] I. J. Goodfellow, J. Pouget-Abadie, M. Mirza, B. Xu, D. Warde-Farley, S. Ozair, A. Courville, and Y. Bengio, "Generative adversarial networks," in *NeurIPS*, 2014.
- [26] R. A. Yeh, Z. Liu, D. B. Goldman, and A. Agarwala, "Semantic facial expression editing using autoencoded flow," *arXiv*, 2016.
- [27] H. Ding, K. Sricharan, and R. Chellappa, "Exprgan: Facial expression editing with controllable expression intensity," in *AAAI*, 2018.
- [28] T. Park, J.-Y. Zhu, O. Wang, J. Lu, E. Shechtman, A. A. Efros, and R. Zhang, "Swapping autoencoder for deep image manipulation," in *NeurIPS*, 2020.
- [29] B. Hu, Z. Zheng, P. Liu, W. Yang, and M. Ren, "Unsupervised eyeglasses removal in the wild," *IEEE Transactions on Cybernetics*, 2020.
- [30] Y. Shen, J. Gu, X. Tang, and B. Zhou, "Interpreting the latent space of gans for semantic face editing," in *CVPR*, 2020.
- [31] D. Cozzolino, G. Poggi, and L. Verdoliva, "Recasting residual-based local descriptors as convolutional neural networks: An application to image forgery detection," in *IH and MMSEC 2017 - Proceedings of the 2017 ACM Workshop on Information Hiding and Multimedia Security*, 2017.
- [32] J. Fridrich and J. Kodovsky, "Rich models for steganalysis of digital images," *IEEE Transactions on Information Forensics and Security*, 2012.
- [33] D. Afchar, V. Nozick, J. Yamagishi, and I. Echizen, "MesoNet: A compact facial video forgery detection network," in *2018 IEEE International Workshop on Information Forensics and Security (WIFS)*, 2018.
- [34] P. Zhou, X. Han, V. I. Morariu, and L. S. Davis, "Two-Stream Neural Networks for Tampered Face Detection," in *ICCVW*, 2017.
- [35] H. H. Nguyen, J. Yamagishi, and I. Echizen, "Capsule-forensics: Using Capsule Networks to Detect Forged Images and Videos," in *ICASSP, IEEE International Conference on Acoustics, Speech and Signal Processing - Proceedings*, 2019.
- [36] C. Szegedy, W. Liu, Y. Jia, P. Sermanet, S. Reed, D. Anguelov, D. Erhan, V. Vanhoucke, and A. Rabinovich, "Going deeper with convolutions," in *CVPR*, 2015.
- [37] C. Szegedy, V. Vanhoucke, S. Ioffe, J. Shlens, and Z. Wojna, "Rethinking the inception architecture for computer vision," in *CVPR*, 2016.
- [38] S. Sabour, N. Frosst, and G. E. Hinton, in *Dynamic routing between capsules*, 2017.
- [39] M. Du, S. Pentyala, Y. Li, and X. Hu, "Towards Generalizable Forgery Detection with Locality-aware AutoEncoder," in *CIKM*, 2020. [Online]. Available: <http://arxiv.org/abs/1909.05999>
- [40] K. Wang, X. Peng, J. Yang, D. Meng, and Y. Qiao, "Region Attention Networks for Pose and Occlusion Robust Facial Expression Recognition," *IEEE Transactions on Image Processing*, 2020.
- [41] S. Li and W. Deng, "A Deeper Look at Facial Expression Dataset Bias," *IEEE Transactions on Affective Computing*, 2020.
- [42] Y. Mirsky and W. Lee, "The Creation and Detection of Deepfakes: A Survey," *arxiv*, 2020.
- [43] E. Real, A. Aggarwal, Y. Huang, and Q. V. Le, "Regularized evolution for image classifier architecture search," in *AAAI*, 2019.
- [44] C. Liu, L.-C. Chen, F. Schroff, H. Adam, W. Hua, A. L. Yuille, and L. Fei-Fei, "Auto-deeplab: Hierarchical neural architecture search for semantic image segmentation," in *CVPR*, 2019.
- [45] G. Ghiasi, T.-Y. Lin, and Q. V. Le, "Nas-fpn: Learning scalable feature pyramid architecture for object detection," in *CVPR*, 2019.
- [46] W. Zhang, J. Fang, X. Wang, and W. Liu, "Efficientpose: Efficient human pose estimation with neural architecture search," *arXiv*, 2020.
- [47] D. Song, C. Xu, X. Jia, Y. Chen, C. Xu, and Y. Wang, "Efficient residual dense block search for image super-resolution," in *AAAI*, 2020.
- [48] B. Zoph, V. Vasudevan, J. Shlens, and Q. V. Le, "Learning transferable architectures for scalable image recognition," in *CVPR*, 2018.
- [49] Y. Qian, G. Yin, L. Sheng, Z. Chen, and J. Shao, "Thinking in Frequency: Face Forgery Detection by Mining Frequency-aware Clues," in *ECCV*, 2020.
- [50] P. Liu, S. Han, Z. Meng, and Y. Tong, "Facial expression recognition via a boosted deep belief network," in *IEEE Conference on Computer Vision and Pattern Recognition*, 2014.
- [51] Matthias Niessner, "Face2Face: Real-time Face Capture and Reenactment of RGB Videos (CVPR 2016 Oral) - YouTube," in *CVPR*, 2016.
- [52] J. Thies, M. Zollhöfer, and M. Nießner, "Deferred neural rendering: Image synthesis using neural textures," in *siggraph*, 2019.
- [53] "https://github.com/marekkowalski/faceswap," 2018.
- [54] "https://github.com/deepfakes/faceswap," 2018.
- [55] J. Fridrich and J. Kodovsky, "Rich models for steganalysis of digital images," *IEEE Transactions on Information Forensics and Security*, 2012.
- [56] D. Cozzolino, G. Poggi, and L. Verdoliva, "Recasting residual-based local descriptors as convolutional neural networks: an application to image forgery detection," in *Proceedings of the 5th ACM Workshop on Information Hiding and Multimedia Security*, 2017.
- [57] B. Bayar and M. C. Stamm, "A deep learning approach to universal image manipulation detection using a new convolutional layer," in *Proceedings of the 4th ACM Workshop on Information Hiding and Multimedia Security*, 2016.
- [58] N. Rahmouni, V. Nozick, J. Yamagishi, and I. Echizen, "Distinguishing computer graphics from natural images using convolution neural networks," in *2017 IEEE Workshop on Information Forensics and Security (WIFS)*, 2017.

- [59] D. Afchar, V. Nozick, J. Yamagishi, and I. Echizen, "Mesonet: a compact facial video forgery detection network," in *2018 IEEE International Workshop on Information Forensics and Security (WIFS)*, 2018.
- [60] Z. Chen and H. Yang, "Attentive Semantic Exploring for Manipulated Face Detection," *arXiv*, 2021.